Theoretical evidence of the observed kinetic order dependence on temperature during the N_2O decomposition over Fe-ZSM-5†

Hazar Guesmi,‡*[a] Dorothee Berthomieu,*[a] Bryan Bromley,[b] Bernard Coq[a] and Lioubov Kiwi-Minsker*[b]

Received 11th September 2009, Accepted 22nd December 2009
First published as an Advance Article on the web 28th January 2010
DOI: 10.1039/b918954h

The characterization of Fe/ZSM5 zeolite materials, the nature of Fe-sites active in N_2O direct decomposition, as well as the rate limiting step are still a matter of debate. The mechanism of N_2O decomposition on the binuclear oxo-hydroxo bridged extraframework iron core site $[Fe^{II}(\mu\text{-}O)(\mu\text{-}OH)Fe^{II}]^+$ inside the ZSM-5 zeolite has been studied by combining theoretical and experimental approaches. The overall calculated path of N_2O decomposition involves the oxidation of binuclear Fe^{II} core sites by N_2O (atomic α-oxygen formation) and the recombination of two surface α-oxygen atoms leading to the formation of molecular oxygen. Rate parameters computed using standard statistical mechanics and transition state theory reveal that elementary catalytic steps involved into N_2O decomposition are strongly dependent on the temperature. This theoretical result was compared to the experimentally observed steady state kinetics of the N_2O decomposition and temperature-programmed desorption (TPD) experiments. A switch of the reaction order with respect to N_2O pressure from zero to one occurs at around 800 K suggesting a change of the rate determining step from the α-oxygen recombination to α-oxygen formation. The TPD results on the molecular oxygen desorption confirmed the mechanism proposed.

1. Introduction

There are environmental and economical stakes for the use of nitrous oxide as an efficient and selective oxidizing reactant in some chemical processes.[1,2] In early work it was claimed that some Fe-exchanged zeolites are highly efficient for the low temperature hydroxylation of aromatics.[3,4] These discoveries gave rise to a large amount of studies about the nature of the active iron and oxygen species formation, and about the mechanism of the N_2O decomposition. In spite of intensive research, the debate is still open about the nuclearity of active iron sites (for a review see ref. 5 and 6), which may impact the mechanism. Depending on the iron content, the preparation mode and activation conditions, a wide distribution of various iron species can be present in the catalyst. Based on kinetics, spectroscopic and modeling studies, mono- and binuclear iron–oxo species have been proposed as the potential active sites rather than clustered oxide species.[5,6] Modeling approaches play a crucial role due to the unusually low content of active iron species (around 3×10^{18} sites g^{-1})[7] preventing univocal spectroscopic experimental assignments. Indeed a detailed knowledge of a mechanism occurring between reactants and solids can be reached by combining energetic and kinetic of elementary steps with a macroscopic description of the reaction. To obtain precise information about the elementary steps in heterogeneous catalytic reaction, it is necessary to get fundamental theoretical description of the electronic structure and the potential energy surface (PES) on which the reaction takes place. Such a description can be reached using a quantum mechanics (QM) approach. A combined approach based on density functional theory (DFT) and on transition state theory (TST) calculations of rate constants was performed for the N_2O decomposition in order to analyse the microscopic behaviour of each elementary step. Regarding kinetics and mechanism, either N_2O dissociation or O_2 desorption have been suggested as the rate determining step in the overall process.[8–17] From DFT modeling of the N_2O decomposition on $Z^-[Fe\text{–}O\text{–}Fe]^{2+}Z^-$ of Fe–ZSM-5, Hansen *et al.*[9] proposed that O_2 desorption is fast, and the rate determining state would be N_2O dissociation, in agreement with the experimentally observed first-order dependence of the N_2O decomposition rate with respect to N_2O pressure. In contrast, from temporal analysis of products (TAP) and steady-state kinetic study, molecular oxygen formation (α-oxygen recombination) has been proposed as the rate limiting step.[7,15] Similar conclusions have been made by us from N_2O decomposition modeling on $Z^-[Fe\text{-}(\mu\text{-}O)(\mu\text{-}OH)\text{-}Fe]^+$ binuclear iron core species.[17] The decomposition of two nitrous oxide molecules into two dinitrogen and one dioxygen molecules

[a] *MACS, Institut Charles Gerhardt, UMR 5253 CNRS/ENSCM/UM2/UM1, Ecole Nationale Supérieure de Chimie de Montpellier, France. E-mail: hazar.guesmi@upmc.fr, dorothee.berthomieu@enscm.fr*
[b] *Ecole Polytechnique Fédérale de Lausanne, GGRC-ISIC-EPFL, Station 6, CH-1015, Lausanne, Switzerland. E-mail: lioubov.kiwi-minsker@epfl.ch*

† Electronic supplementary information (ESI) available: Experimental determination of the reaction order: N_2O decomposition data. See DOI: 10.1039/b918954h

‡ Present address: Laboratoire de Réactivité de Surface, UMR 7197 Université Pierre et Marie Curie, 4 place Jussieu, 75252 Paris, France

via the following sequence steps (reactions (1)–(8)) has been examined:[17]

$$Z^-[Fe(\mu\text{-}O)(\mu\text{-}OH)Fe]^+ + N_2O_{(g)} \rightarrow Z^-[N_2O\text{–}Fe(\mu\text{-}O)(\mu\text{-}OH)Fe]^+ \quad (1)$$

$$Z^-[N_2O\text{–}Fe(\mu\text{-}O)(\mu\text{-}OH)Fe]^+ \rightarrow Z^-[O\text{–}Fe(\mu\text{-}O)(\mu\text{-}OH)Fe]^+ + N_{2(g)} \quad (2)$$

$$Z^-[O\text{–}Fe(\mu\text{-}O)(\mu\text{-}OH)Fe]^+ + N_2O_{(g)} \rightarrow Z^-[O\text{–}Fe(\mu\text{-}O)(\mu\text{-}OH)Fe\text{–}ON_2]^+ \quad (3)$$

$$Z^-[O\text{–}Fe(\mu\text{-}O)(\mu\text{-}OH)Fe\text{–}ON_2]^+ \rightarrow Z^-[O\text{–}Fe(\mu\text{-}O)(\mu\text{-}OH)Fe\text{–}O]^+ + N_{2(g)} \quad (4)$$

$$Z^-[O\text{–}Fe(\mu\text{-}O)(\mu\text{-}OH)Fe\text{–}O]^+ \rightarrow Z^-[O\text{–}Fe(\mu\text{-}O\text{–}O)(\mu\text{-}OH)Fe]^+ \quad (5)$$

$$Z^-[O\text{–}Fe(\mu\text{-}O\text{–}O)(\mu\text{-}OH)Fe]^+ \rightarrow Z^-[O_{2(singlet)}\text{–}Fe(\mu\text{-}O)(\mu\text{-}OH)Fe]^+ \quad (6)$$

$$Z^-[O_{2(singlet)}\text{–}Fe(\mu\text{-}O)(\mu\text{-}OH)Fe]^+ \rightarrow Z^-[O_{2(triplet)}\text{–}Fe(\mu\text{-}O)(\mu\text{-}OH)Fe]^+ \quad (7)$$

$$Z^-[O_{2(triplet)}\text{–}Fe(\mu\text{-}O)(\mu\text{-}OH)Fe]^+ \rightarrow Z^-[Fe(\mu\text{-}O)(\mu\text{-}OH)Fe]^+ + O_{2(g)(triplet)} \quad (8)$$

N_2O reacts at low temperature and decomposes into N_2 and atomic oxygen (α-oxygen) adsorbed on each iron in a highly stable $Z^-[O\text{–}Fe\text{-}(\mu\text{-}O)(\mu\text{-}OH)\text{-}Fe\text{–}O]^+$ intermediate. This process is followed by atomic oxygen migration which occurs through the highest free energy barrier. This result suggested that the latter process (reaction (5)) is the rate determining step of the overall kinetics. The catalyst is regenerated after α-oxygen recombination and molecular oxygen desorption. However, a temperature dependence of the elementary steps has been suggested, which may explain the literature controversy on the overall process.[17]

On that account, the aim of the present study is a deep investigation *via* kinetic experiments and modeling of elementary steps, the temperature dependence of the rate constants of the N_2O decomposition on $[Fe\text{-}(\mu\text{-}O)(\mu\text{-}OH)\text{-}Fe]^+$ in Fe-ZSM-5. We first report a DFT analysis of the microscopic behaviours of elementary steps of the N_2O decomposition over a binuclear iron complex in Fe-ZSM-5 for a large temperature range. Then, experimental investigation of the kinetics has been carried out at low (< 600 K) and high (> 800 K) temperatures in combination with temperature programmed desorption (TPD) to confirm the predicted temperature dependence of the observed kinetic order and to evidence that the μ-oxo–μ-hydroxo bridging binuclear iron complex can be considered as the active site in Fe-ZSM-5 zeolites.

2. Methodology

2.1 Computational details

Mechanistic and energetic aspects of the N_2O decomposition over $Z^-[Fe\text{-}(\mu\text{-}O)(\mu\text{-}OH)\text{-}Fe]^+$ using the B3LYP/TZVP method and a cluster approach have been previously reported.[17] A complete energy profile of N_2 and O_2 formation was

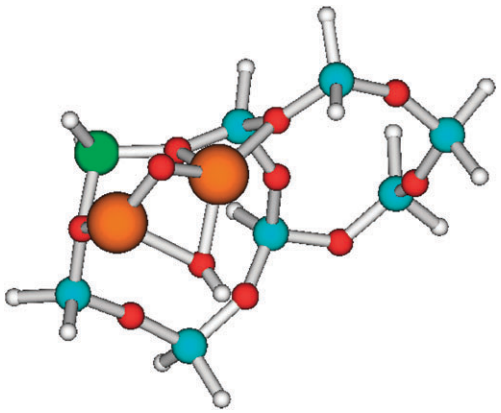

Fig. 1 $[Fe\text{-}(\mu\text{-}O)(\mu\text{-}HO)\text{-}Fe]^+Z^-$ cluster model with the formula $Fe_2O_{10}Al_1Si_7H_{15}$ in which Z^- is two five member rings from the main channel of ZSM-5 zeolite. Largest balls are Fe and smallest balls are H. Ball sizes are larger for Al than for Si, than for O.

proposed. In the present study, reaction rate calculations of elementary processes have been performed using the same method and the same cluster model (see Fig. 1).[17] Overall equilibrium constants and reaction rate constants were computed using standard statistical mechanics and conventional TST.[18,19] The partition functions for reactants and transition states (TS) were calculated using the harmonic approximation. For all gaseous species participating in the reaction *i.e.* $N_2O_{(g)}$, $N_{2(g)}$ and $O_{2(g)}$, translational (q_{tran}), rotational (q_{rot}), vibrational (q_{vib}), and electronic (q_{el}) contributions of the partition function were considered. Since the zeolite cluster representing the catalytic active site is a part of a solid, transitional and rotational partition functions were assumed to be equal in the reactant, transition state and product. Thus, only the vibrational and electronic contributions of the partition function were included.

For a reaction

$$A \xrightarrow{k_{AB}} B$$

in one spin potential energy surface the reaction rate constant is given by:

$$k_{AB} = \frac{kT}{h}\frac{Q_{TS}}{Q_A}\exp\left(-\frac{E_a}{kT}\right) \quad (1)$$

with a partition function Q for N non-interacting identical particles written as:

$$Q = \frac{q^N}{N!} \quad (2)$$

and a partition function, q, for a single molecule defined as a product of terms:

$$q = q_{trans}q_{rot}q_{vib}q_{el} \quad (3)$$

k is the Boltzmann constant, T the temperature, h the Planck constant and E_a the activation energy of the reaction including zero point energy (ZPE) correction.

For elementary processes in which the spin state changes during reaction, eqn (1) cannot be applied to determine spin-surface crossing rates. The minimum energy crossing point (MECP) is located in the region where two spin surfaces

(low and high) cross and thus, it is not a stationary point.[20,21] For MECP, the framework of TST was used assuming that the partition functions of MECP and reactant state are identical except for the electronic energy. Consequently,

$$k_{\text{low}\rightarrow\text{high}} = \frac{kT}{h}\exp\left(-\frac{\Delta E}{kT}\right) \quad (4)$$

where ΔE is the electronic energy difference between MECP and reactant. The same approach was used for the computation of adsorption rates and desorption processes on the same PES (eqn (5)).

$$k_{\text{ads/des}} = \frac{kT}{h}\exp\left(-\frac{\Delta E}{kT}\right) \quad (5)$$

Calculation details of rate parameters and estimation errors can be found elsewhere.[22,23]

2.2 Experimental

Catalyst preparation. The ZSM-5 zeolites used in the present study were prepared by hydrothermal synthesis described elsewhere.[24] Two different samples with an iron concentration of 1200 ppm: HZSM-$5_{1200\text{Fe};40\text{Si/Al}}$ (28% of active iron) and HZSM-$5_{1200\text{Fe};120\text{Si/Al}}$ (27% of active iron) with Si/Al = 40 and 120, respectively and a sample with an iron concentration of 2300 ppm: HZSM-$5_{2300\text{Fe};42\text{Si/Al}}$ (26% of active iron) with Si/Al = 42 were used in this study. Typically, tetraethylorthosilicate (TEOS; Fluka, 98%) was added to an aqueous solution of tetrapropylammonium hydroxide (TPAOH; Fluka, 20% in water) used as a template, $NaAlO_2$ (Riedel-de Haën, Na_2O 40–45%, Al_2O_3 50–56%). The molar ratios of the components were TEOS : TPAOH : $NaAlO_2$: H_2O = 0.8 : 0.1 : 0.016–0.032 : 33. The mixture was stirred for 3 h at room temperature, and the clear gel obtained was transferred to a stainless-steel autoclave lined with PTFE and kept at 180 °C for 2 days. The product was filtered, washed with deionised water and calcined in air at 550 °C for 12 h. The zeolite was then converted into the H-form by an exchange with a NH_4NO_3 aqueous solution (0.5 M) and subsequent calcination at 550 °C for 3 h. The catalysts were activated by steaming (H_2O partial pressure of 0.3 bar, He flow rate 50 mL min^{-1}) at 550 °C for 4 h and also by heating at 1050 °C in He (50 mL min^{-1}) for 1 h. The particles of samples obtained have a specific area around 340–370 m^2 g^{-1}, a pore volume around 0.21–0.27 cm^3 g^{-1} and a diameter around 63–80 μm.

Reaction kinetics study. Reaction kinetics was studied using a Micromeritics AutoChem 2910 analyzer. The gases were supplied by Carbogas, Switzerland (purities > 99.998%). The NO_x content in N_2O was below 2 ppm. The following peaks were monitored simultaneously by mass-spectrometer: 4 (He), 18 (H_2O), 28 (N_2, N_2O), 30 (NO, N_2O), 32 (O_2), 40 (Ar), 44 (N_2O) and 46 (NO_2) m/z. The set-up, as well as a fused silica capillary connected to the mass-spectrometer, was heated up to 110 °C. Before the reaction runs, the activated catalysts were pre-treated in He (50 mL min^{-1}) at 1050 °C for 1 h, then cooled down to the selected temperature. In the experiments a mixture of 2 vol% N_2O/2 vol% Ar in He was normally used unless it was desired to vary the N_2O concentration. For these experiments, the mixtures containing 1.3, 1 and 0.7 vol% of N_2O were prepared by dilution of the original mixture with He. Argon was always added as an inert internal tracer.

Catalyst characterization. The chemical composition of the catalysts was determined by atomic absorption spectroscopy (AAS) *via* a Shimadzu AA-6650 spectrometer. The samples were dissolved in boiling aqua regia containing several drops of HF.

The specific surface areas (SSA) of the catalyst were measured using N_2 adsorption–desorption at 77 K *via* a Sorptomatic 1990 instrument (Carlo Erba) employing the BET method while the Dollimore–Heal method was applied for the calculation of pore volume. The particles diameter was estimated by sieving.

Temperature programmed desorption was used to analyze the species present on the catalyst surface by monitoring oxygen and NO_x. 0.4 g of pre-activated catalyst was placed into the reactor and pretreated in He at 1273 K for 30 min. After this, the catalyst was cooled to 523 K and put in contact with N_2O for different time from 10 s to 5 min. TPD measurements were performed in He (20 mL (STP) min^{-1}) at heating rate of 30 °C min^{-1}. The gaseous composition was monitored up to 1000 K.

Results and discussion

Calculated rate constants of the N_2O decomposition

The overall reaction path of N_2O decomposition over $Z^-[Fe\text{-}(\mu\text{-}O)(\mu\text{-}OH)\text{-}Fe]^+$ within the eight elementary steps (reaction (1)–(8)) has been considered.[17]

Steps 1 and 3 (reaction (1) and (3)) correspond to the reversible adsorption of gas phase N_2O over the first and the second iron ions of the active complex, respectively. In steps 2 and 4 (reaction (2) and (4)) the dissociation of each of two adsorbed nitrous oxide species occurs, leading to the release of two equivalents of gaseous nitrogen and the formation of two surface α-oxygen species. The recombination of the atomic α-oxygen occurs through step 5 (reaction (5)), where one surface oxygen atom migrates, *via* the μ-O bridge, from one iron atom to the other, followed by step 6 (reaction (6)) forming adsorbed O_2. As the molecular oxygen desorbs in its triplet state, a spin change corresponding to a surface crossing from the singlet to the triplet state takes place through step 7 (reaction (7)). Finally, the last step of the catalytic cycle is the O_2 molecule desorption (reaction (8)).

The calculated kinetic rate constants of these 8 elementary steps have been investigated over a large temperature range: from 300 K to 1000 K (Table 1). In Fig. 2 the kinetic constants of each elementary step, as [ln(k)] against the reciprocal temperature, are reported.

The analysis of the calculated kinetic rate constants as a function of temperature reveals two major trends:

(i) At temperatures below 800 K, the lowest calculated rate constant corresponds to the O migration occurring inside the iron core complex (reaction (5)). The reaction rates of steps 4 and 8 (reaction (4) and (8)) are also low, but O_2 formation remains slower than N_2 formation, with a difference between rate constants of at least one order of magnitude.

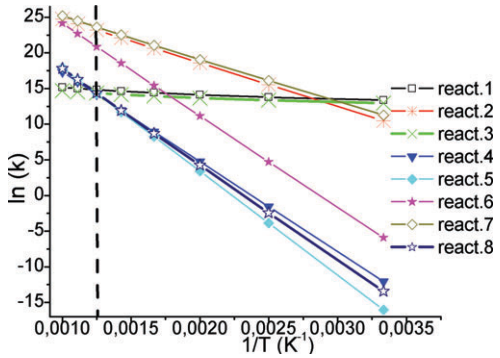

Fig. 2 Evolution of rate constants as a function of the reciprocal temperature of the eight elementary reaction steps of the computed N_2O decomposition pathway over $[Fe\text{-}(\mu\text{-oxo})(\mu\text{-hydroxo})\text{-}Fe]^+Z^-$ site, calculated within the harmonic approximation and using standard statistical mechanics and TST.

In contrast, steps 1 and 3 (reaction (1) and (3)) corresponding to N_2O adsorption on iron are fast.

Above 800 K, the kinetic behaviour changes drastically: the adsorption process becomes the slowest elementary steps controlling the overall reaction (reaction (1) and (3)). The kinetic rate constants of all steps are greater than 10^6 s^{-1}, suggesting a very fast N_2O decomposition process. It is worth noting that while all the rate constants increase with temperature, the rates of adsorption are not sensitive to temperature and remain nearly constant whatever the temperature (Table 1).

This theoretical investigation reveals the strong dependency of unimolecular step rate constants and evidences a switch in the rate-determining step occurring around 800 K.

Let us note that generally by inspecting simply the magnitude of the rate constants of elementary steps it is not possible to draw any conclusions about the overall reaction kinetics. Microkinetic modelling is often done, but it may give erroneous conclusions because of several simplifying assumptions.[26]

In order to understand the kinetic behaviour of our model active site, we compared qualitatively the results calculated in the present study with those calculated over another type of binuclear iron site. Hansen *et al.*[9] have performed a detailed reaction mechanism for N_2O decomposition over the binuclear $Z^-[Fe\text{–}O\text{–}Fe]^{2+}Z^-$ active sites and reported rate parameters calculated at the same level of theory. In addition, these authors have developed a consistent microkinetic model[23] on the bases of calculated rate parameters showing that the slowest process is the N_2O dissociation step, which is also the rate-determining of the catalytic reaction. They assign this result to be consistent with the observed first order dependence of the N_2O decomposition rate with respect to N_2O pressure. But this is true only at high temperatures and does not correspond to the experimentally observed zero order

Table 1 DFT computed enthalpies ΔH (kcal mol^{-1}), activation energies $E^{\ddagger}$ (kcal mol^{-1}) and rate constants parameters (prefactors A and kinetic rate constants k in s^{-1} bar^{-1}) for nitrous oxide decomposition reaction elementary steps (reaction (1)–(8)) over the μ-oxo–μ-hydroxo bridging binuclear iron complex in Fe-ZSM-5 at temperature range from 300 to 1000 K

React.	ΔH and $E^{\ddagger}$/kcal mol^{-1}; A and k constants/$s^{-1}bar^{-1}$	T/K 300	400	500	600	700	800	900	1000
(1)	$\Delta H_1 = -6.8$								
	$E_1^{\ddagger} = 0.0$								
	A_1	6.31E+05	9.67E+05	1.35E+06	1.78E+06	2.25E+06	2.76E+06	3.29E+06	3.86E+06
	k_1	6.31E+05	9.67E+05	1.35E+06	1.78E+06	2.25E+06	2.76E+06	3.29E+06	3.86E+06
(2)	$\Delta H_2 = -27.1$								
	$E_2^{\ddagger} = 11.5$								
	A_2	9.02E+12	1.13E+13	1.32E+13	1.48E+13	1.61E+13	1.72E+13	1.80E+13	1.88E+13
	k_2	3.56E+04	5.62E+06	1.20E+08	9.30E+08	4.03E+09	1.21E+10	2.85E+10	5.65E+10
(3)	$\Delta H_3 = -4.2$								
	$E_3^{\ddagger} = 0.0$								
	A_3	4.13E+05	6.26E+05	8.70E+05	1.14E+06	1.44E+06	1.76E+06	2.09E+06	2.45E+06
	k_3	4.13E+05	6.26E+05	8.70E+05	1.14E+06	1.44E+06	1.76E+06	2.09E+06	2.45E+06
(4)	$\Delta H_4 = -13.5$								
	$E_4^{\ddagger} = 24.3$								
	A_4	3.32E+12	4.34E+12	5.17E+12	5.81E+12	6.30E+12	6.69E+12	6.99E+12	7.23E+12
	k_4	5.79E-06	2.08E-01	1.14E+02	7.67E+03	1.54E+05	1.46E+06	8.42E+06	3.40E+07
(5)	$\Delta H_5 = 6.0$								
	$E_5^{\ddagger} = 28.4$								
	A_5	6.14E+13	7.62E+13	8.58E+13	9.20E+13	9.60E+13	9.86E+13	1.00E+14	1.02E+14
	k_5	1.08E-07	2.07E-02	3.02E+01	3.86E+03	1.22E+05	1.62E+06	1.21E+07	6.04E+07
(6)	$\Delta H_6 = -13.6$								
	$E_6^{\ddagger} = 24.3$								
	A_6	1.56E+15	2.32E+15	3.08E+15	3.83E+15	4.55E+15	5.27E+15	5.97E+15	6.66E+15
	k_6	2.71E-03	1.11E+02	6.82E+04	5.05E+06	1.12E+08	1.15E+09	7.18E+09	3.13E+10
(7)	$\Delta H_7 = -3.7$								
	$E_7^{\ddagger} = 10.8$								
	A_7	6.25E+12	8.33E+12	1.04E+13	1.25E+13	1.46E+13	1.67E+13	1.88E+13	2.08E+13
	k_7	8.00E+04	1.00E+07	1.91E+08	1.41E+09	6.04E+09	1.83E+10	4.39E+10	8.93E+10
(8)	$\Delta H_8 = 24.8$								
	$E_8^{\ddagger} = 25.5$								
	A_8	6.25E+12	8.33E+12	1.04E+13	1.25E+13	1.46E+13	1.67E+13	1.88E+13	2.08E+13
	k_8	1.45E-06	8.79E-02	6.86E+01	6.01E+03	1.50E+05	1.71E+06	1.15E+07	5.35E+07

at low temperatures. In contrast with our results, they do not predict a change of the reaction rate order with temperature. The rate constants over the $Z^{-}[Fe(\mu\text{-}O)(\mu\text{-}OH)Fe]^{+}$ active site calculated herein allow us to explain the change of the observed reaction kinetics order from zero at low temperature to one at higher temperatures with respect to N_2O pressure.[13]

These aspects have been investigated in detail experimentally and the results obtained are presented below.

Reaction order under steady-state conditions

The kinetics of N_2O decomposition was studied at different temperatures in the range 573–823 K and the reaction orders were measured under steady state conditions. At temperatures above 773 K, the reaction rate is very fast and the steady state is reached within a few seconds. This is not the case at low temperature where the reaction is very slow. Moreover, the reaction rate increases in time and this autocatalytic effect is assigned to the accumulation of NO_x surface species.[5,11,25] Its formation comes from the interaction between N_2O and the atomic α-oxygen labeled as $(O)_{Fe}$ (reaction (9)).

$$N_2O + (O)_{Fe} \rightarrow 2NO_{ads} + (\,)_{Fe} \qquad (9)$$

This process is slow and, depending on the reaction temperature, it takes up to 2 h to attain the steady state.[7] Therefore, the N_2O decomposition was first performed at 603 K and then cooled down to the desired temperature. In this case the steady state is rapidly reached.

It is worth noting that NO_x surface species do not occupy the sites involved in the α-oxygen formation, $(\,)_{Fe}$, and so, can't affect the interaction of N_2O with the catalytic surface.

Moreover, the total amount of NO_x formed is about two orders of magnitude smaller as compared to the total oxygen loaded (Fig. 4). Compared to a mechanism without involvement of NO, we suppose that NO would increase the reaction order in N_2O. If the reaction order is close to zero even in the presence of NO, the same must be true for the reaction pathway without NO, which was modelled by DFT. Therefore, we supposed that the comparison of DFT calculations for the iron α-sites with experimental data in terms of the reaction order at low temperature is still valid.

To determine the reaction order, the N_2O decomposition was studied varying concentrations of N_2O (2.0, 1.3, 1.0 and 0.75%) at the total gas flow rate constant. (see the ESI for details†).

The measurements were done for different samples ($HZSM\text{-}5_{1200Fe;40Si/Al}$ and $HZSM\text{-}5_{1200Fe;120Si/Al}$) and the results are presented in Fig. 3. The reaction order is close to zero at 573 K, increases with temperature and reaches one at temperature above 773 K.

That the reaction order is close to zero at low temperature demonstrates that there is no dependence of the overall reaction rate on the concentration of N_2O in the gas-phase. This experimental result is in line with the calculations predicting a fast surface saturation by atomic oxygen of which migration/recombination is not influenced by N_2O concentration. At high temperatures the observed kinetic order is unity and the overall rate becomes directly proportional to the concentration of N_2O. This result confirms a change of the rate limiting step within the mechanism of the N_2O decomposition (from the O_2 step to the atomic α-oxygen formation step) as predicted by the above calculations.

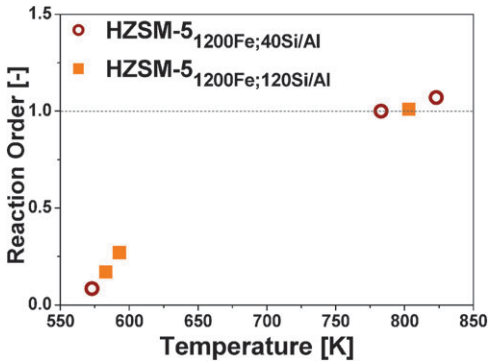

Fig. 3 Reaction order at steady state during N_2O decomposition over $HZSM\text{-}5_{1200Fe;40Si/Al}$ and $HZSM\text{-}5_{1200Fe;120Si/Al}$ at different temperatures.

Oxygen recombination studied by TPD

It is well known that during N_2O decomposition a small fraction of NO_x is formed which accelerates oxygen recombination.[11,25] Due to the presence of NO_x at the catalyst surface, the mechanism of oxygen recombination is more complex at low temperature than the mechanism based on reaction (1)–(8). It is also well known that NO_x formation (reaction (9)) is very slow and the amount of NO adsorbed on the catalyst is negligible at short contact times. Oxygen recombination was studied by TPD after the N_2O decomposition at 573 K for 5 min (Fig. 4) and 10 s (Fig. 5) on $HZSM\text{-}5_{2300Fe;42Si/Al}$. Fig. 4 shows a maximum of O_2 desorption at 663 K. In this case, a small amount of NO after the oxygen peak is observed. In Fig. 5 the amount of NO formed during N_2O decomposition is too low to be detected by mass spectrometry and the maximum of the O_2 desorption peak is shifted to 759 K. The shift of the maximum of the O_2 desorption peak at low temperatures observed in the presence of NO_x indicates a facilitation of atomic oxygen migration/recombination induced by NO_x, but this temperature neither exceeded 760 K with or without NO_x.

Therefore, we can conclude that in the most unfavourable conditions (no NO_x on the surface) direct oxygen recombination

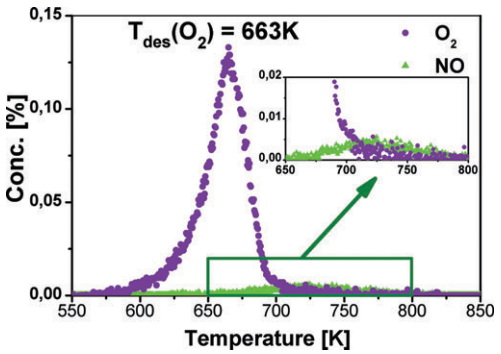

Fig. 4 TPD profiles of $HZSM\text{-}5_{2300Fe;42Si/Al}$ after contacting with N_2O for 5 min at 523 K.

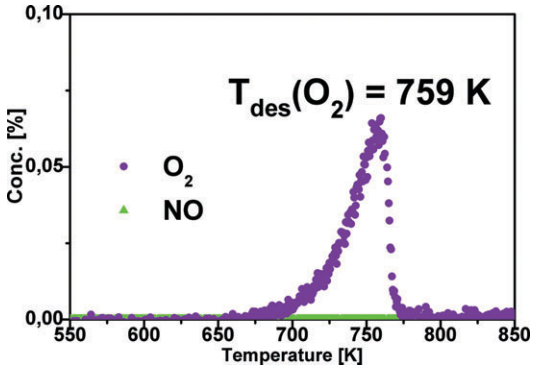

Fig. 5 TPD profiles of HZSM-$5_{2300Fe;42Si/Al}$ after contacting with N_2O for 10 s at 523 K.

takes place at temperatures below 800 K and cannot be the rate determining step at reaction temperatures >800 K. This result confirms that the steps of atomic oxygen deposition (reaction (1)) and (reaction (3)) become rate determining, in line with the DFT calculations (Fig. 2).

Conclusion

A combined experimental and DFT study of the N_2O decomposition to N_2 and O_2 on [Fe-(μ-oxo)(μ-hydroxo)-Fe]$^+Z^-$ active sites revealed a change of rate limiting step in the reaction mechanism with temperature increase from 300 K to 1000 K. This change is due to the strong temperature dependence of elementary steps predicted from DFT calculations. Based on steady state kinetic experiments and temperature-programmed desorption (TPD), it was shown that at low temperatures atomic oxygen (saturating iron active α-sites at the catalyst surface) are the most abundant intermediates and that their recombination/desorption is the rate-limiting step of the overall catalytic cycle, in agreement with theoretical findings. Finally, as predicted from DFT investigations, at temperature higher than 800 K atomic oxygen formation becomes the rate limiting step resulting in the observed first order kinetics with respect to N_2O.

Acknowledgements

The present work was financially supported by the European network of excellence IDECAT NMP-CT-2005-011730 WP.7.3, by the Swiss National Science Foundation and by the convention 07CARN00301 of the Institute CARNOT "Chimie Environnementale et Développement Durable—Chimie Montpellier". Calculations were carried out on the IBM SP4 computers of the CINES (Centre Informatique National de l'Enseignement Supérieur) in Montpellier (France) and of the IDRIS (Institut des Ressources en Informatique Scientifique) in Orsay (France).

References

1 G. I. Panov, K. A. Dubkov and E. V. Starokon, *Catal. Today*, 2006, **117**, 148.
2 V. N. Parmon, G. I. Panov, A. Uriarte and A. S. Noskov, *Catal. Today*, 2005, **100**, 115.
3 G. I. Panov, V. I. Sobolev and A. S. Kharitonov, *J. Mol. Catal.*, 1990, **61**, 85.
4 M. Gubelmann and P. J. Tirel, Preparation of phenol by oxidation of benzene, in *Eur. Pat. Appl.*, Rhone-Poulenc Chimie SA, France, Ep, 1989, p. 4.
5 G. D. Pirngruber, P. K. Roy and R. Prins, *Phys. Chem. Chem. Phys.*, 2006, **8**, 3939.
6 A. Zecchina, M. Rivallan, G. Berlier, C. Lamberti and G. Ricchiardi, *Phys. Chem. Chem. Phys.*, 2007, **9**, 3483.
7 L. Kiwi-Minsker, D. A. Bulushev and A. Renken, *Catal. Today*, 2004, **91–92**, 165.
8 A. Heyden, B. Peters, A. T. Bell and F. J. Keil, *J. Phys. Chem. B*, 2005, **109**, 1857.
9 N. Hansen, A. Heyden, A. T. Bell and F. J. Keil, *J. Phys. Chem. C*, 2007, **111**, 2092.
10 F. Kapteijn, G. Marban, J. Rodriguez-Mirasol and J. A. Moulijn, *J. Catal.*, 1997, **167**, 256.
11 D. A. Bulushev, L. Kiwi-Minsker and A. Renken, *J. Catal.*, 2004, **222**, 389.
12 C. Sang, B. H. Kim and C. R. F. Lund, *J. Phys. Chem. B*, 2005, **109**, 2295.
13 L. Kiwi-Minsker, D. A. Bulushev and A. Renken, *Catal. Today*, 2005, **110**, 191.
14 K. Sun, H. Xia, E. Hensen, R. Van Santen and C. Li, *J. Catal.*, 2006, **238**, 186.
15 E. V. Kondratenko and J. Perez-Ramirez, *J. Phys. Chem. B*, 2006, **110**, 22586.
16 E. V. Kondratenko and J. Perez-Ramirez, *Catal. Today*, 2007, **119**, 243.
17 H. Guesmi, D. Berthomieu and L. Kiwi-Minsker, *J. Phys. Chem. C*, 2008, **112**, 20319.
18 W. K. Hall, X. Feng, J. Dumesic and R. Watwe, *Catal. Lett.*, 1998, **52**, 13.
19 S. C. Tucker and D. G. Truhlar, Dynamical formulation of transition state theory: variational transition states and semiclassical tunneling, in *New Theor. Concepts Understanding Org. React.*, 1989, vol. 267, p. 291.
20 J. N. Harvey, M. Aschi, H. Schwarz and W. Koch, *Theor. Chem. Acc.*, 1998, **99**, 95.
21 J. N. Harvey and M. Aschi, *Phys. Chem. Chem. Phys.*, 1999, **1**, 5555.
22 A. Heyden, PhD thesis, Hamburg University of Technology, 2005.
23 N. Hansen, A. Heyden, A. T. Bell and F. J. Keil, *J. Catal.*, 2007, **248**, 213.
24 I. Yuranov, D. A. Bulushev, A. Renken and L. Kiwi-Minsker, *J. Catal.*, 2004, **227**, 138.
25 G. Mul, J. Perez-Ramirez, F. Kapteijn and J. A. Moulijn, *Catal. Lett.*, 2001, **77**, 7.
26 B. Temel, H. Meskine, K. Reuter, M. Scheffler and H. Metiu, *J. Chem. Phys.*, 2007, **126**, 204711.

